DOI: 10.15669/pnst.4.276

Progress in Nuclear Science and Technology
Volume 4 (2014) pp. 276-279

ARTICLE

Optimum shielding structure for the wall of medical LINAC facility

Kazuaki Kosako[a*], Koji Oishi[a], Takashi Nakamura[a] and Yoshiaki Kiyanagi[b]

[a]*Shimizu Corporation, 4-17 Etchujima 3-Chome, Koto-ku, Tokyo, 135-8530, Japan;* [b]*Hokkaido University, Kita 13, Nishi 8, Kita-ku, Sapporo, Hokkaido, 060-8628, Japan*

When considering the space limit of high energy LINAC facility in a hospital, the design of shielding wall is strongly required to optimize the wall thickness. Shielding wall usually consists of concrete, and iron plate is sometimes added in concrete to decrease the wall thickness. We investigated the optimum design of the shielding wall in medical LINAC facility by simulation. The calculations were carried out by the three-dimensional Monte Carlo code, MCNP5. The electron energy used in this investigation is 28 MeV. In the calculations, the wall thickness was fixed to 100 cm from the viewpoint of durability and reliability and the cost to build the shielding wall. In the shielding wall consisting of iron and concrete, the suitable configuration was found to have 40-50 cm-thick iron at the front side. But it was insufficient to achieve the required attenuation rates of 2 x 10^{-6} and 5 x 10^{-8} for effective neutron and photon doses, respectively. We further searched the optimum combination of shielding materials to get the most efficient attenuation profile and finally obtained the optimum arrangement of 100 cm thick shielding wall having the multi-layered structure of iron 40 cm, polyethylene 10 cm, iron 20 cm, lead 10 cm, polyethylene 10 cm, and concrete 10 cm in this order. In order to investigate the shielding capability of this multi-layered shielding wall, the neutron and photon dose rates were measured using the 45 MeV electron linear accelerator of Hokkaido University to verify the MCNP5 calculated results. The MCNP5 calculation was found to give good accuracy within 30% for the multi-layered shielding structure.

Keywords: electron; linear accelerator; medical LINAC; Monte Carlo; MCNP5; shielding design; dose rates; photoneutron; shielding wall thickness

1. Introduction

The mortality rate of cancer in Japan is about 30% in 2010 and has been increasing. At present, the ratio of radiation therapy for the cancer patients in Japan is about 25% [1,2]. Electron linear accelerators (LINAC) are widely used in radiation cancer therapy due to many clinical cases and cost benefit, and more than 900 LINAC are being operated in Japan [3]. Recently, the electron energy of greater than 10 MeV is gradually increasing with the upgrade of irradiation method and the expansion of applicability. LINAC with high functionality has been developed to apply to IMRT (Intensity Modulated Radiation Therapy), IGRT (Image Guided Radiation Therapy), and CyberKnife. When the electron energy is greater than 10 MeV, neutrons are produced through photonuclear reactions by bremsstrahlung photons. The shielding calculation including photoneutron reactions is very important in the shielding design of electron LINAC facilities, especially for shielding wall, maze and door.

The shielding design has not been investigated sufficiently for medical LINAC with the electron energy of greater than 10 MeV. Therefore here in this study, we investigated the optimum structure of shielding wall of the LINAC facility using the 3-dimensional Monte Carlo transport code, MCNP5 [4] which has been widely used to the shielding calculation. We performed to find the optimum combination and configuration of shielding materials under the constraint condition of 100 cm thick shielding wall, considering the space limit in a hospital. In order to verify the calculated accuracy of MCNP5 with cross section data, we executed the experiments of neutron and photon dose rates using the 45 MeV electron linear accelerator of Hokkaido University.

2. Calculation of optimum shielding structure

2.1. Calculation condition

In the simulation, we used the MCNP5 code, which has the function of electron, photon and neutron transport calculation, electron-photon cascade calculation, and photoneutron production calculation. The cross section data libraries used in MCNP5 calculations are EL3 for electron-photon cascade reactions, MCPLIB04 for photon interaction,

*Corresponding author. Email: k.kosako@shimz.co.jp

FSXLIB-J33 for neutron reactions, and LA150U for photonuclear reactions [5,6].

In the MCNP5 calculation, an electron beam was injected normally to the copper target (2 cm thickness and 4 by 4 cm in area) fixed at 20 cm behind the beam extraction window (30 μm thickness of titanium). The form of electron beam was approximated as a Gaussian spatial distribution of 1 cm radius as a standard deviation. The peak energy of electron beam was 28 MeV and the full width at half maximum of the spectra was 4 MeV. The copper were selected as a target using widely in the medical LINAC. The calculation condition is the same as in the experiment at the 45 MeV electron linear accelerator of Hokkaido University as described later [7,8]. The tallies were the point detectors to estimate the photon and neutron fluxes. These were set on the front and rear surfaces and inside positions in the shielding wall. The flux-to-effective dose conversion factor was cited from the data given in ICRP-74 [9].

2.2. Condition of shielding wall

In the conventional shielding design, the wall generally consists of concrete and iron, and the wall thickness is from 150 to 300 cm with or without iron plate (15- to 70-cm thicknesses) inserted into concrete [10]. From our practical design calculation, the attenuation rates for effective neutron and photon doses required to shielding wall of 18 MeV electron LINAC of 21.6 μA electron beam current and 150 hr operation during 3 months were 2 x 10^{-6} and 5 x 10^{-8}, respectively, in order to satisfy the dose limit in Japan outside the shielding wall (8.6 [μSv h^{-1}] = 1.3 [mSv 3-months^{-1}]).

In this study, the 100 cm thick shielding wall is the final goal as described before, and under this constraint condition, we investigated the optimum combination of shielding materials and configurations which has the same attenuation rates as above for higher electron energy of 28 MeV. The further requirement in the construction for the materials of shielding wall is cost, durability and reliability.

3. Simulation of optimum shielding wall

3.1. Location and thickness of iron plate

We first examined the most suitable location and thickness of iron plate fixed in the concrete wall as the conventional shield structure. The location of iron plate of 20 cm thickness was changed from the front surface into the concrete wall and calculated the effective neutron and photon dose rate as a function of wall depth. It was clarified that the photon attenuation behind 100 cm thick wall (20 cm thick iron and 80 cm thick concrete) is almost independent to the location of iron plate, while on the other hand, the neutron attenuation is most efficient when iron plate is placed in the front side to the target. This might be that photoneutron production can be effectively suppressed by iron.

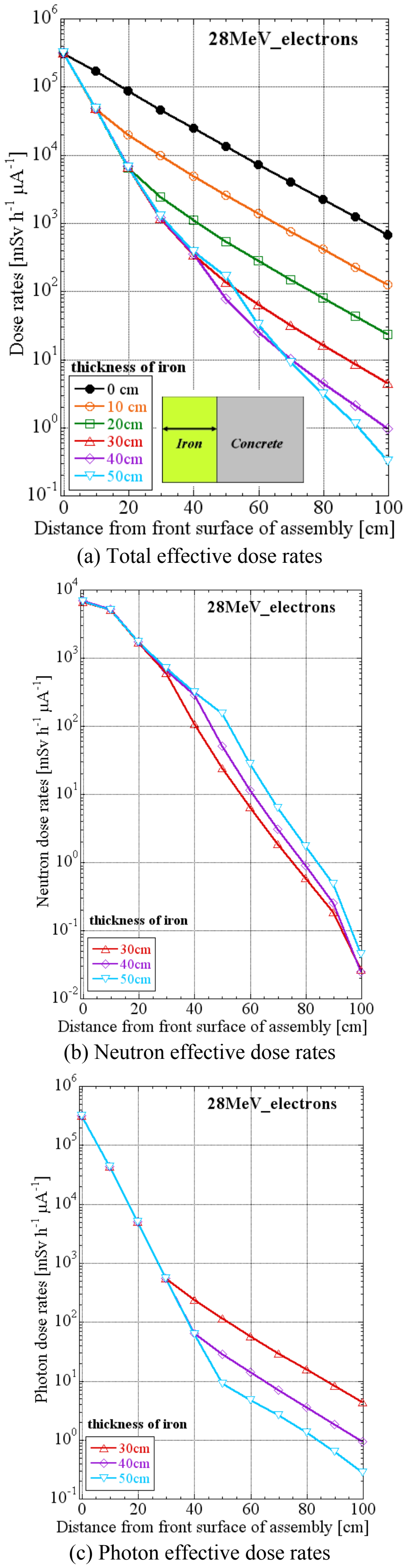

Figure 1. Effective dose rates of total, neutrons and photons by the survey calculations to get the optimum iron thickness, in the case of 28 MeV electrons.

We then surveyed the total effective dose of neutrons and photons to get the optimum iron thickness, as shown in **Figure 1**. As shown in Figures 1(b) and 1(c), as for the thickness of iron plate at the front surface from 0 to 50 cm, neutrons are most effectively shielded for 30 to 40 cm thickness under the condition of 100 cm thick iron and concrete shield, and for photons the thicker the iron shield, the lower the photon dose. Considering the total effective dose of neutrons and photons, iron thickness of 50 cm placed on the front surface of concrete shield gives the smallest value as shown in Figure 1(a). Nevertheless, the attenuation rates of doses still do not satisfy the condition of 2 x 10^{-6} and 5 x 10^{-8} for neutrons and photons, respectively, as shown in Figure 1(b) and 1(c). The total effective dose rate curve of 50 cm thick iron shows the different behavior from others, because the contribution of the neutron dose becomes dominant.

3.2. Optimum configuration of shielding structure

We therefore performed further survey calculations to find the optimum combination of shielding materials with 100 cm thickness in total and finally clarified the optimum structure of 40 cm thick iron. 10 cm thick polyethylene, 20 cm thick iron, 10cm thick lead, 10 cm thick polyethylene, and 10cm thick concrete in this order. The simulated results are shown in **Figure 2** as a function of shield depth. The results could achieve the effective dose attenuation rates of 1.0 x 10^{-7} for neutrons and 1.0 x 10^{-8} for photons, which are lower than 2 x 10^{-6} and 5 x 10^{-8} shown with the dashed lines in Figure 2, respectively.

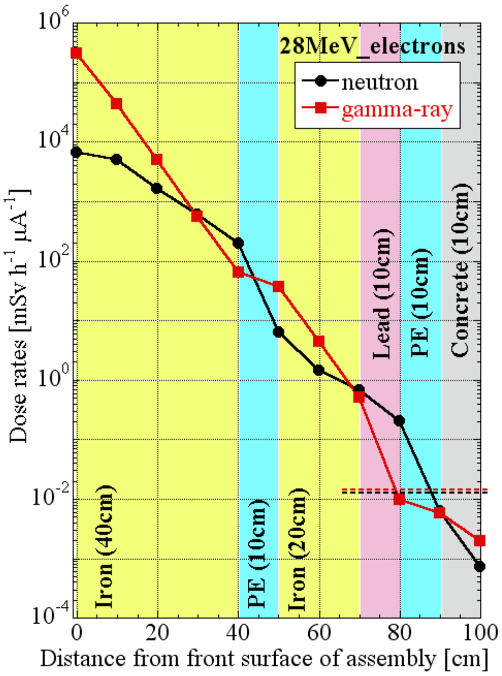

Figure 2. Calculated neutron and photon dose rate distributions in optimum combination of shielding materials with 100 cm thickness irradiated by 28 MeV electrons. (The dashed line means the effective dose attenuation rates, 2 x 10^{-6} for neutrons and 5 x 10^{-8} for photons.)

4. Experimental results

4.1. Experimental procedure

In order to verify the calculated accuracy of MCNP5 with cross section data, we executed the experiments of neutron and photon dose measurements using the 45 MeV electron linear accelerator of Hokkaido University. The experimental condition of the target is the same as the calculation described in 2.1.

Figure 3 gives the experimental geometry. The shielding material has a plate of 40 x 40 cm^2 and the total thickness of the shield assembly is 94 cm, not 100 cm. The thicknesses of materials are 36 cm iron, 10 cm polyethylene, 18 cm iron, 10 cm lead, 10 cm polyethylene, and 10 cm concrete. The shielding structure is the same as given in 3.2. The distance from the target to the shield is 100 cm and the dosimeters used in this experiment are OSL (Optically Stimulated Luminescence, Al_2O_3) by Nagase-Landauer Co. [11] and Glass Dosimeter by Chiyoda Technol. Co. [12] for photons and SSTD (Solid State Track Detector) [13] by both companies for neutrons. The electron beam current was 4.2 μA and the irradiation times were 100 and 1000 seconds in two times of experiments.

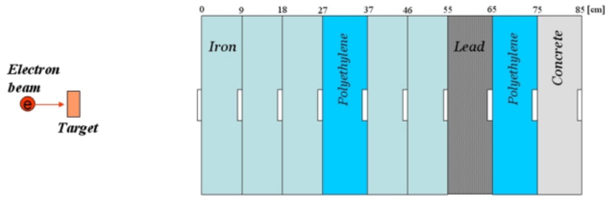

Figure 3. Experimental arrangement of the copper target and the multi-layer shielding assembly.

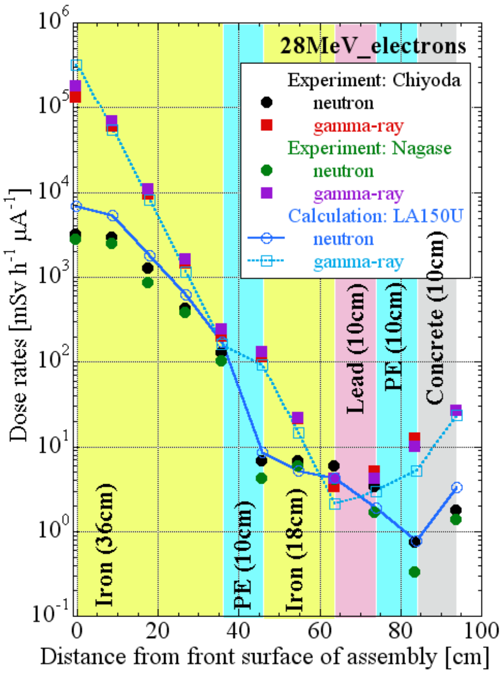

Figure 4. Neutron and photon dose rate distributions of calculated and measured results in the experimental multi-layer shielding assembly irradiated by 28 MeV electrons.

4.2. Comparison with calculated results

The comparison between calculated and measured results using the optimum configuration of shielding materials is shown in **Figure 4**. The agreement between calculation and experiment is very good within 30% even after about 10^{-5} order of magnitude decrease, although beyond 60 cm depth, the dose rates slightly increase due to the effect of room scattering under the experimental condition. In the front surface region, the calculated results overestimate the experimental values. The difference of neutron dose rates is because LA150U gives overestimation of the photoneutron production with iron. The difference of photon dose rates is because the dosimeters have low sensitivity to high energy photons generated at the target. From this comparison, it was confirmed that the MCNP5 calculation gives enough accurate results. We could finally realize the optimum multi-layer shielding wall of 100 cm thickness for use in limited space in a hospital.

5. Conclusion

In the conventional shielding wall consisting of concrete and iron, the optimum shielding structure for high energy LINAC is that the 40 to 50 cm thickness iron plate is arranged to front side.

We found the optimum multi-layer shielding wall of 100 cm thickness for use at a limited space in a hospital, by using the MCNP5 calculation. It was confirmed by the comparison with the experimental result. The calculated accuracy of MCNP5 is within 30% for the shielding design of high energy LINAC facility.

References

[1] JASTRO Database Committee, Japanese structure survey of radiation oncology in 2005 (First report), *J. Japan Soc. Ther. Radiol. Oncol.,* 19 (2007), pp. 181-192.

[2] Y. Mochimaru, Y. Ohno, H. Numasaki and T. Teshima, The change of treatment resources at the radiotherapy facilities in Osaka; based on the Japanese Society of Therapeutic Radiology and Oncology Survey, *IT Healthcare,* 4 (2009), pp. 80-83. [in Japanese]

[3] Japan Radioisotope Association, *Statistics of the Use of Radiation in Japan,* (2010).

[4] X-5 Monte Carlo Team, *MCNP – A General Monte Carlo N-Particle Transport Code, Version 5,* LA-UR-03-1987, Los Alamos National Laboratory, (2003).

[5] RSICC, *Data Libraries for MCNP5,* CCC-710/MCNP, Oak Ridge National Laboratory, (2003).

[6] K. Kosako, N. Yamano, T. Fukahori, K. Shibata and A. Hasegawa, *The Libraries FSXLIB and MATXSLIB Based on JENDL-3.3,* JAERI-Data/Code 2003-011, Japan Atomic Energy Research Institute, (2003).

[7] K. Kosako, K. Oishi, T. Nakamura, M. Takada, K. Sato, T. Kamiyama and Y. Kiyanagi, Angular Distribution of bremsstrahlung from copper and tungsten targets bombarded by 18, 28, and 38 MeV Electrons, *J. Nucl. Sci. Technol.* 47 (2010), pp. 286-294.

[8] K. Kosako, K. Oishi, T. Nakamura, M. Takada, K. Sato, T. Kamiyama and Y. Kiyanagi, Angular distribution of photoneutrons from copper and tungsten targets bombarded by 18, 28, and 38 MeV Electrons, *J. Nucl. Sci. Technol.* 48 (2011), pp. 227-236.

[9] ICRP, *Conversion Coefficients for use in Radiological Protection against External Radiation,* ICRP Publication 74, Annals of the ICRP 26(3/4), Pergamon Press, Oxford, (1995).

[10] P.H. McGinley, *Shielding Techniques for Radiation Oncology Facilities,* Medical Physics Pub. Corp., (2002), ISBN 1930524072.

[11] A. Suzuki and M. Ito, *Characteristics of OSL Dosimeters,* JAERI-Tech 2000-089, Japan Atomic Energy Research Institute, (2000). [in Japanese]

[12] D. Maki, N. Juto and Y. Koguchi, Performance of the glass badge dosimeter system, *Proc. of the Second Asian Oceanic Congress for Radiat. Prot. (AOCRP-2)* (2006), pp. 604-607.

[13] H. Ohguchi, Development and estimation of wide-energy range personal neutron dosimeter using solid state track detector, Kobe University, Doctoral thesis (2009).